Available online at www.sciencedirect.com
ScienceDirect
Ceramics International 37 (2011) 3583–3590
CERAMICS INTERNATIONAL
www.elsevier.com/locate/ceramint

Densification behaviour and properties of manganese oxide doped Y-TZP ceramics

S. Ramesh [a,*], M. Amiriyan [b], S. Meenaloshini [b], R. Tolouei [b], M. Hamdi [a], J. Purboloksono [a], W.D. Teng [c]

[a] *Centre of the Advanced Manufacturing & Material Processing (AMMP), Department of Engineering Design and Manufacture, Faculty of Engineering University of Malaya, 50603 Kuala Lumpur, Malaysia*
[b] *Ceramics Technology Lab., University Tenaga Nasional, 4009 Kajang, Malaysia*
[c] *Ceramics Technology Group, SIRIM Berhad, 40911 Shah Alam, Malaysia*

Received 19 April 2011; received in revised form 2 June 2011; accepted 9 June 2011
Available online 15 June 2011

Abstract

The effect of employing a short sintering holding time of 12 min as compared to that of the commonly employed holding time of 120 min (2 h) on the properties of undoped and 1 wt% manganese oxide (MnO_2)-doped Y-TZP ceramics were studied. Sintering studies was conducted over the temperature range of 1150–1600 °C. Bulk density, Young's modulus, Vickers hardness and fracture toughness tests were carried out on the sintered samples. The results revealed that the 12 min sintering holding time was effective in promoting densification of the 1 wt% MnO_2-doped Y-TZP without sacrificing tetragonal phase stability or mechanical properties and incurring grain growth. Microstructure investigation by using the scanning electron microscope (SEM) of the fracture MnO_2-doped Y-TZP samples which was subjected to rapid quenching in liquid nitrogen revealed distinct microstructural features believed to be associated with the presences of a transient liquid phase during sintering. A sintering mechanism was subsequently proposed to explain the densification behaviour of MnO_2-doped Y-TZP ceramics.

Keywords: C. Mechanical properties; Engineering ceramics; Y-TZP; Sintering additives; Sintering holding time

1. Introduction

Yttria-stabilised tetragonal zirconia polycrystals or subsequently known as Y-TZP has been tailored to take full advantage of the transformation toughening effect of the tetragonal grains [1,2]. These ceramics are characterised by excellent strength above 800 MPa [3,4], high toughness (>10 $MPam^{1/2}$) [5,6] and good wear resistance [7] which makes it ideal for a host of applications including metal cutting tools, sharp edges for knifes and scissors, sandblasting nozzles, and biomedical implant [8–13]. Y-TZP is also used as an electrolyte for ionic conduction application such as oxygen sensors [14,15] and as an oxide-ion conducting electrolyte for solid oxide fuel cell devices operating at approximately 1000 °C [16–18]. Additionally, Y-TZP ceramics have been shown to have superior shock resistance over other ceramics such as alumina and mullite [19,20], thus rendering this material suitable for high temperature applications [21–24].

In the transformation toughening phenomenon, the tetragonal to monoclinic phase transition in the vicinity of a propagating crack tip is accompanied by an approximately 4% volume expansion. As a result, compressive stress is generated at the crack tip thereby making it difficult for further crack advancement [25]. Transformation toughening in Y-TZPs can induce strength and toughness much higher than those of most other monolithic ceramics and approaching those of low strength metals [3,8,26]. The requirement for enhance transformation toughening necessitate the retention of tetragonal grains in the metastable state, i.e. the grains would respond immediately to the stress such as that induced by a propagating crack and transform to the monoclinic symmetry. Amongst the various approaches employed by researchers in order to achieve a metastable tetragonal structure, the control of the sintering parameters and the use of sintering additives have been found to be most viable and economical method.

---

* Corresponding author. Tel.: +60 3 7967 7671; fax: +60 3 7967 5330.
E-mail address: ramesh79@um.edu.my (S. Ramesh).

0272-8842/$36.00 © 2011 Elsevier Ltd and Techna Group S.r.l. All rights reserved.
doi:10.1016/j.ceramint.2011.06.014

The use of transition metal oxide such as copper oxide as a sintering aid in Y-TZP ceramics has been shown by numerous researchers to be beneficial in enhancing sintering and improving densification at relatively low temperatures and short holding times. Many workers such as Kimura et al. [27], Ramesh et al. [28], Hwang and Chen [29], Xue [30], Seidensticker et al. [31], Hendrix et al. [32], Lawson et al. [33] and Ran et al. [34,35], have indeed suggested that a liquid phase was 'active' during the sintering of the copper-doped zirconia ceramic. Previous study [36] has demonstrated the usefulness of manganese oxide (MnO_2) in aiding sintering of Y-TZP, however the actual role of this additive in aiding densification was not resolved. As such, this research focused on the densification behaviour and properties of 1 wt% MnO_2-doped Y-TZP powders by controlling the sintering, particularly the sintering holding time prior to cooling to room temperature.

2. Experimental procedure

2.1. Sample preparation

The as-received 3 mol% yttria-stabilized zirconia starting powder used in this work was manufactured by Kyoritsu Ltd., Japan. The powder had a total impurity concentration of about 0.1 wt%, with SiO_2, Fe_2O_3, TiO_2 and Al_2O_3 as the major impurities. The starting Y-TZP powder is designated hereafter as undoped. In the present work, 1 wt% of high purity manganese oxide (α-MnO_2) powder (BDH, United Kingdom) was mixed with the Y-TZP powder by wet milling in ethanol. This composition was chosen based on the outcome of previous work reported elsewhere [36]. The mixture was milled for 1 h, after which the slurry was dried at 60 °C in oven for 12 h. The dried filtered cake was then crushed and sieved through a 212 μm mesh stainless steel sieve to obtain ready-to-press MnO_2-doped Y-TZP powder.

Disc (20 mm diameter × 5 mm thickness, each weighing 2.5 g) and rectangular bar (32 mm × 13 mm × 6 mm, each weighing 3 g) green samples were uniaxially compacted at 3 MPa and subsequently cold isostatically pressed at 200 MPa. The green samples were subjected to pressureless sintering under ambient condition, using a standard rapid heating furnace (ModuTemp, Australia), at various temperatures ranging from 1150 °C to 1600 °C. Two different sintering holding times (the time at which the samples would be soaked at the required temperature during sintering) was evaluated, i.e. the conventional 2 h, hereafter shall be known as 120-min hold samples and a shorter holding time equivalent to 1/10th of the conventional value, i.e. 12 min was chosen for the study, hereafter shall be known as 12-min hold samples. In both cases, the heating and cooling rates during sintering were kept standard at 10 °C/min based on previous work [37]. All sintered samples were polished to a 1 μm surface finish prior to properties evaluation.

2.2. Characterization

The bulk densities of sintered compacts were determined by the water immersion technique based on the Archimedes principle using a standard (Mettler Toledo Balance AG204) densi-meter. In addition relative density was calculated based on the 6.09 g/cm^3 for Y-TZP. The Young's modulus of the rectangular samples was measured by sonic resonance instrument (Grindosonic; MK5, Belgium). The instrument permits determination of the resonant frequency of a specimen by monitoring and estimating the vibrational harmonics of the sample by using a transducer; tapping was used to induce physical vibrations in the sample. The modulus of elasticity is calculated using the experimentally determined resonant frequencies, according to standard test method [38]. The Vickers indentation method (Future Tech., Japan) was used on polished samples to determine Vickers hardness and fracture toughness (K_{Ic}). The indentation load was kept constant at 10 kg for 10 s. The K_{Ic} corresponding to the indentation is calculated from equation derived by Niihara et al. [39]. Average values of three measurements were used for each test and the error was found to be less than 1%.

The phase analysis of undoped and 1 wt% MnO_2 doped samples was carried out by X-ray diffraction (XRD) using low-angle $\{1\,1\,1\}c,t$, $\{1\,1\,1\}m$ and $\{1\,1\,\bar{1}\}m$ reflections which enabled the quantitative determination of the monoclinic phase content present in the material. A Rigaku diffractometer was used with Cu-Kα radiation operating at 35 kV/15 mA in step mode with a 0.02° 2θ step and a step scan of 0.5°/min over the 2θ range 27–36° which covers the monoclinic (m) and tetragonal/cubic (t + c) related {1 1 1} peaks. The relationship established by Toraya et al. [40] which took into account the total intensity of the unresolved (c) and (t) peaks were employed to determine the relative amounts of monoclinic zirconia. In this work, for the cubic phase measurement, a 0.02° 2θ step and a count time of 35.5 s per step over the 2θ range 72–76° which covers the cubic related {0 0 4} phase was employed. The volume fraction of the cubic phase was then estimated by using the relationship of Paterson and Stevens [41].

The average tetragonal grain size of the samples was measured on polished surface using the line intercept method [42]. For this purpose, the samples were thermally etched at a temperature 50 °C below the sintering temperature, using a ramp rate of 10 °C/min and holding time of 30 min. The etched surfaces were examined using a Philips XL30 scanning electron microscope (SEM).

In the quest to obtain evidence of the presence of transient liquid phase, an attempt was made to trap (if any) the liquid phase that was present during sintering. For this study, selected Y-TZP samples were heated in the furnace up to the sintering temperature, hold for 5 min to stabilize the temperature and then the samples were subjected to rapid quenching in liquid nitrogen. The fracture surfaces of these samples were subsequently examined using the SEM.

3. Results and discussion

3.1. Powder characteristics

The XRD analysis of the as-received Y-TZP powder exhibited ~85% tetragonal (t) and ~15% monoclinic (m)

Table 1
Properties of undoped and 1 wt% MnO_2-doped Y-TZP powders.

Powders	%(m)	%(t)	Crystallite size (nm)	SSA (m^2/g)
Undoped	15.0	85.0	36	9.76
1 wt% MnO_2-doped	19.2	80.8	36	9.42

phase content. The MnO_2 addition increased the monoclinic (m) phase content of the Y-TZP powder slightly from 15% to 19.2% as given in Table 1. The present of a dual phase microstructure or a composite material is not expected at least for the MnO_2-doped powder in this work. This was confirmed by XRD and SEM analysis of the sintered samples.

Additionally, the specific surface area obtained by the BET method on both powders did not vary significantly. A similar observation was made for the crystallite size measured from peak broadening based on Scherrer's formula [43] for Y-TZP powders taken at the most prominent zirconia peak at $\{1\ 1\ 1\}c,t$, reflection corresponding to diffraction angle $2\theta \approx 30.1^\circ$ as shown in Table 1. These results indicated that the powder properties were not affected by the addition of the dopant.

3.2. Tetragonal phase retention

The 12-min hold sintering cycle was beneficial in controlling the monoclinic (m) and cubic (c) phase development in the doped ceramic, particularly for samples sintered at higher temperatures. The results as shown in Fig. 1 indicated that samples sintered up to 1500 °C composed of fully tetragonal structure. However, a small amount of monoclinic phase (i.e. ~3.3%) was detected in the sample sintered at 1600 °C. This is relatively small as compared to ~48% developed in a similar sample sintered using the 120-min hold sintering cycle. The grain sizes of all samples sintered from 1250 °C onwards are given in Table 2. In general, the results indicated that the addition of MnO_2 did not significantly affect the average tetragonal grain size. However, the microstructure of the 1 wt% MnO_2-doped sample sintered at 1600 °C using the 120-min hold cycle was porous resulting in low density as depicted in Fig. 2.

3.3. Relative density

The effect of sintering temperature on relative density of the undoped and MnO_2-doped Y-TZPs sintered using both sintering cycles are compared as shown in Fig. 2. The results show that for sintering below 1350 °C and regardless of sintering holding time employed, the undoped Y-TZP could not be sintered to above 95% relative density. Additionally, for sintering below 1400 °C, all the 120-min hold sintered samples exhibited higher density than the equivalent 12-min hold sintered samples. However, for sintering above 1400 °C the undoped samples attained almost similar densification regardless of sintering holding time employed.

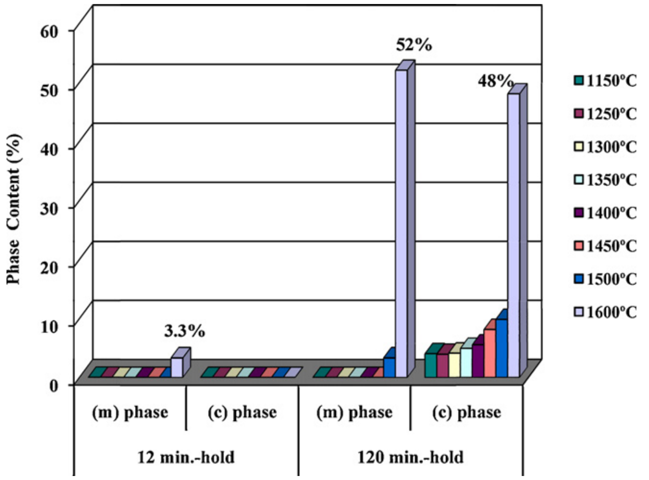

Fig. 1. Comparison between the monoclinic (m) and cubic (c) phase content in the MnO_2-doped Y-TZP samples sintered using different sintering holding times.

In the case of the 1 wt% MnO_2-doped samples, the 12-min hold sintering cycle was found to be beneficial in enhancing the densification of the ceramics, particularly for samples sintered above 1350 °C as shown in Fig. 2. The fact that the short holding time of 12 min prevented the formation of cubic phase in the tetragonal matrix throughout the sintering regime employed and the formation of monoclinic phase in samples sintered at 1500 °C, indicates that the degree of yttria segregation from the tetragonal grain was lower in these samples as compared to that observed for samples sintered using the 120 min SHT cycle [37]. The present results agreed well with the findings of other researchers who employed MnO_2 as a sintering additive in Y-TZP [27,44]. Manganese oxide in the form of MnO_2 and Mn_3O_4 has been shown to be effective in promoting densification of Y-TZP. Kimura et al. [27] reported that doping Y-TZP with 0.3 mol% (~0.21 wt%) MnO_2 allowed almost full densification to proceed at 1200 °C,

Table 2
Average tetragonal grain size (μm) of Y-TZPs as a function of sintering temperature and holding time.

Sintering temperature (°C)	1 wt% MnO_2-doped Y-TZP		Undoped Y-TZP	
	12-min hold	120-min hold	12-min hold	120-min hold
1250	0.13	0.23	0.15	0.24
1300	0.14	0.25	0.17	0.26
1350	0.15	0.29	0.19	0.32
1400	0.17	0.35	0.2	0.38
1450	0.18	0.41	0.21	0.44
1500	0.20	0.50	0.22	0.51
1600	0.25	Porous	0.42	0.73

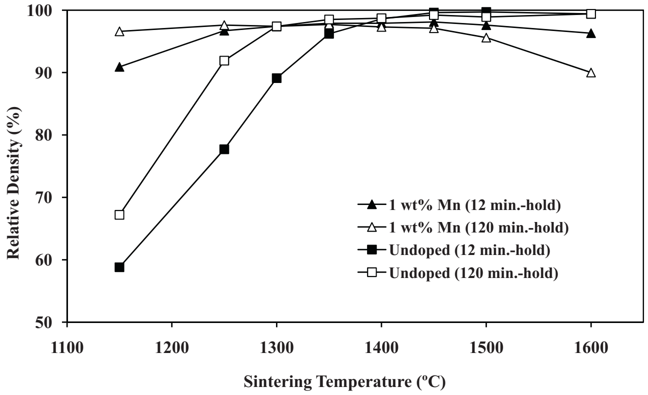

Fig. 2. Relative density variation of undoped and MnO_2-doped Y-TZPs sintered using different sintering holding times.

about 200 °C lower than undoped Y-TZP without incurring any abnormal grain growth.

The beneficial effect of manganese oxide in aiding densification was also observed in other ceramic matrices such as alumina [45], ceria [46] as well as lithium and potassium tantalates ($LiTaO_3$, $KTaO_3$) [47]. Erkalfa et al. [45] observed that alumina with additions of 0.1–0.5 wt% manganese oxide showed marginal improvement in bulk density when sintered at 1550 °C for 1 h. However, the addition of 3 wt% MnO_2 in alumina and sintered at temperatures of 1250–1450 °C for the same holding time recorded 4–9% higher density but this was accompanied by substantial grain growth. Shimada et al. [47] discovered that the addition of 3 wt% of MnO_2 to $LiTaO_3$ resulted in rapid densification even at 1125–1190 °C, leading to relative densities of 85–90% within 30 min compared to 60–62% for the undoped ceramic. Sakka et al. [44] reported that Y-TZP with additions 0.1–0.3 mol% (0.2–0.9 wt%) of Mn_3O_4 yielded relative densities beyond 95% when sintered at 1200 °C when compared to the undoped Y-TZP which only achieved 82% of theoretical density.

3.4. Young's modulus, Vickers hardness and fracture toughness

The effect of sintering temperature and holding time on the Young's modulus (*E*), Vickers hardness and fracture toughness of Y-TZPs are presented in Figs. 3–5, respectively. In general, the Young's modulus trend of both doped and undoped ceramics regardless of sintering conditions was in agreement with the relative density trend as shown in Fig. 2. For the undoped ceramic, samples sintered below 1450 °C using the 120-min hold sintering cycle exhibited higher elastic modulus than that sintered using the 12-min hold sintering cycle. However, both the undoped ceramics attained almost similar *E* values (i.e. ~200–205 GPa) when sintered $\geq$ 1450 °C as shown in Fig. 3.

In the case of the MnO_2-doped Y-TZP, the sample sintered at 1150 °C using the 120-min hold sintering cycle exhibited higher *E* value of 191 GPa as compared to 155 GPa for the 12-min hold sintered sample. However, as the temperature was increased above 1150 °C, MnO_2-doped samples attained almost similar elastic modulus of >200 GPa. The beneficial effect of the short sintering holding time in enhancing the Young's modulus of MnO_2-doped Y-TZP can be seen, particularly for samples sintered at higher temperatures (>1400 °C) where a decline in the *E* values was inevitable for the samples sintered by 120-min hold sintering cycle.

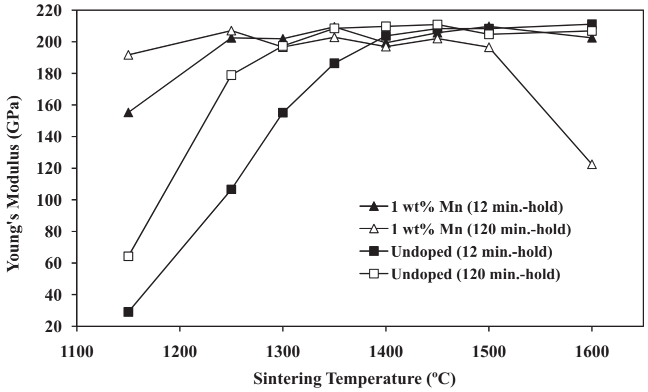

Fig. 3. Young's modulus variation of undoped and MnO_2-doped Y-TZPs as function of sintering temperature.

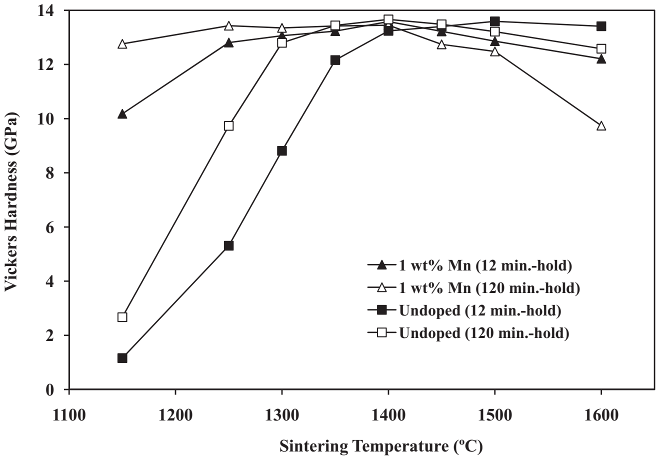

Fig. 4. Influence of sintering parameters on the Vickers hardness of Y-TZPs.

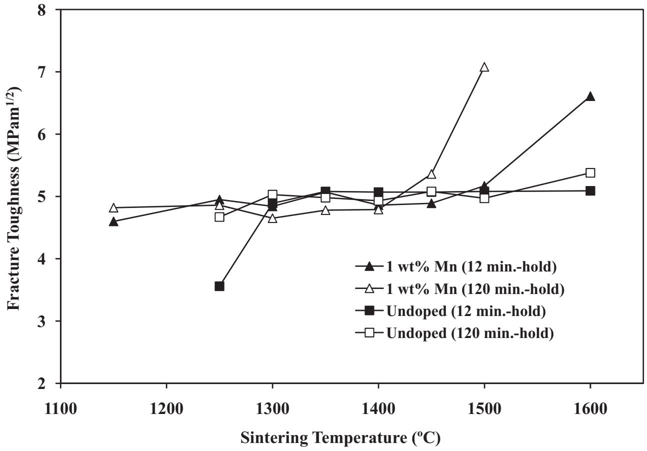

Fig. 5. Fracture toughness variation of undoped and MnO_2-doped Y-TZPs sintered at different temperatures.

A similar effect can be noted for the Vickers hardness variation with respect to sintering temperature and holding times as shown in Fig. 4. The hardness of the undoped Y-TZP sintered below 1400 °C using the 12-min hold sintering cycle was lower than sample sintered using the 120-min hold sintering cycle. However, for sintering above 1400 °C, the hardness of the former was higher than the latter as depicted in Fig. 4. A similar observation was noted for the Vickers hardness trend of the MnO_2-doped ceramics when sintered above 1400 °C. The 12-min hold sintered samples exhibited higher hardness values when compared to their equivalent samples sintered using 120-min hold sintering cycle. This improvement in the Young's modulus and Vickers hardness of the MnO_2-doped Y-TZP when sintered using the 12-min hold sintering cycle could be attributed to the improved densification as well as the high tetragonal phase retention in the zirconia matrix. In general, regardless of dopant additions, the hardness of all the Y-TZPs started to decrease when sintered above 1400 °C. This trend of increasing hardness until a maximum at a certain sintering temperature followed by a continuous decline thereafter with further sintering as seen in the present study is in agreement with the findings of other researchers [36,48,49].

As for the fracture toughness (K_{Ic}), Fig. 5 shows that the sintering holding time has negligible effect on the fracture toughness of the undoped Y-TZP especially when sintered above 1150 °C. This observation was also true for the MnO_2-doped ceramic for up to 1400 °C sintering. However, for sintering above 1400 °C, the 12-min hold sintered ceramics exhibited an increased in fracture toughness.

The comparison between the fracture toughness and tetragonal phase content with respect to sintering temperature for Y-TZP containing 1 wt% MnO_2 sintered under the 12-min hold sintering cycle is shown in Fig. 6. The sharp increase of fracture toughness with decreasing tetragonal phase content is in agreement with the findings of Kim [50], who attributed the huge improvement of K_{Ic} in Y-TZP with Ta_2O_5 and Nb_2O_5 additions to the enhanced transformability of the tetragonal grains.

One possible explanation for the higher K_{Ic} in the MnO_2-doped zirconia could be associated with the tetragonal phase stability in the zirconia matrix. The decrease in (t) phase content in the MnO_2-doped Y-TZP with increasing sintering temperatures as shown in Fig. 6 strongly suggest that the presence of MnO_2 could have triggered a mechanism which caused yttria segregation in the Y-TZP matrix. It can be hypothesized that during sintering, an influx of yttria to certain tetragonal grains will over-stabilize the tetragonal grains, leading to exaggerated grain growth and the formation of yttria-rich cubic phase. The minority grains that suffered severe yttria dissolution would undergo a spontaneous (t) to (m) phase transformation upon cooling to room temperature. This was supported by the small amount of monoclinic phase detected by XRD in the MnO_2-doped samples when sintered at 1500 °C. On the other hand, tetragonal grains with lesser yttria depletion (not below the limit required for phase destabilisation to occur) would still remain in the tetragonal form but in a metastable state. These grains would readily undergo transformation toughening upon Vickers indentation resulting in relatively high values of fracture toughness being recorded as shown in Fig. 5.

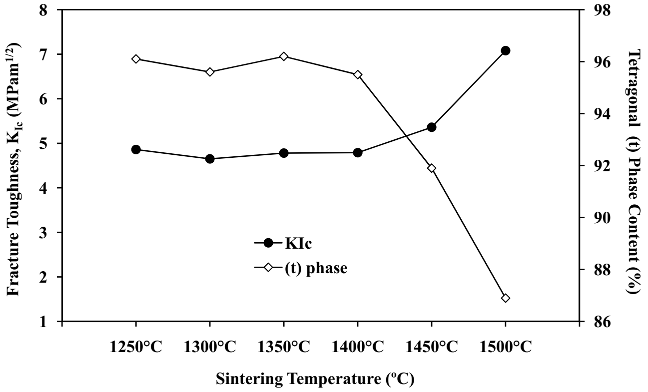

Fig. 6. Variation of fracture toughness and tetragonal phase content of MnO_2-doped Y-TZP as a function of sintering temperature.

4. Microstructural evolution

The microstructural development of MnO_2-doped samples was compared with that of undoped samples quenched in liquid nitrogen from the sintering temperature. Physical inspection of all the samples revealed that cracking was observed mainly for the undoped samples after quenching from temperatures below 1500 °C. However, regardless of sintering temperature, all the MnO_2-doped samples did not exhibit any surface cracking.

The resultant microstructure of fracture surface of the undoped ceramics sintered at 1150 °C and 1350 °C are shown in Figs. 7 and 8, respectively. There was no indication of unusual microstructure or signs of the presence of a glassy phase regardless of firing temperature. Additionally, the EDAX analysis on these samples revealed the presence of mainly Zr

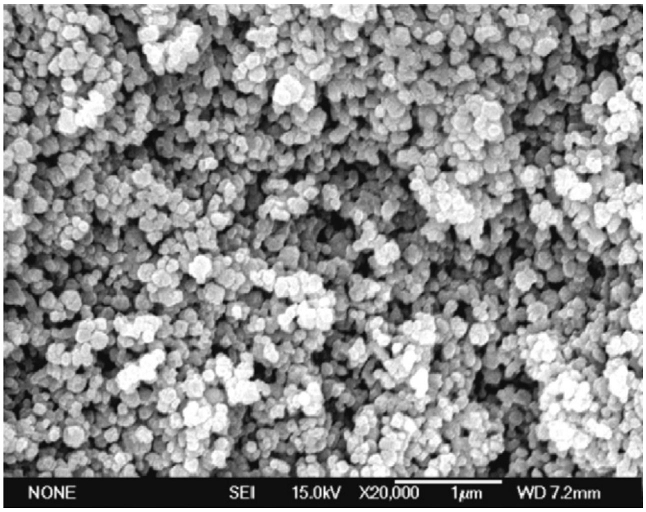

Fig. 7. SEM micrograph of unpolished fracture surface of undoped Y-TZP that was rapidly quenched from 1150 °C revealing no sign of the presences of liquid phase.

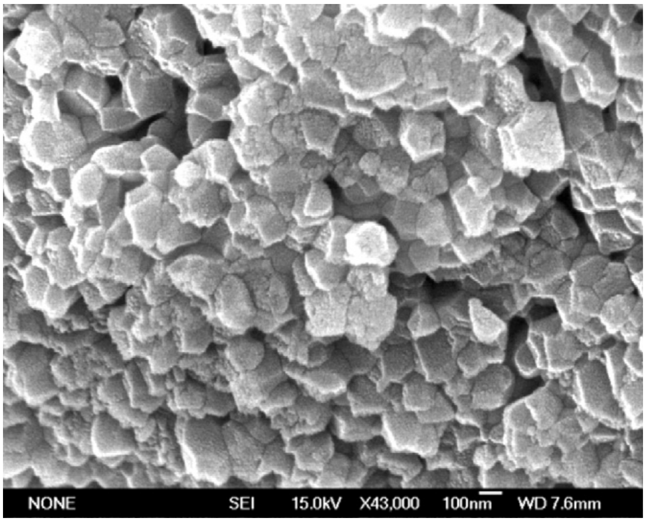

Fig. 8. SEM micrograph of unpolished fracture surface of undoped Y-TZP that was rapidly quenched from 1350 °C.

and Y elements at grain boundaries as well as grain interior. On the other hand, examination performed on the quenched fracture surface of MnO_2-doped Y-TZP fired at 1150 °C and 1350 °C revealed some interesting features. This was evident from the SEM pictures as shown in Figs. 9 and 10. A general comparison between Fig. 9 with that of Fig. 7 revealed that the MnO_2-doped Y-TZP was denser than the undoped ceramic when fired at 1150 °C. This result further confirmed that Mn doping enhances the densification rate in comparison to the undoped samples. The microstructural examination of the quenched MnO_2-doped Y-TZP revealed unique features, believed to be associated with the presences of a transient liquid phase, such as the rounded pore formation and the rounding of the grain boundaries as shown in Fig. 10.

The EDAX analysis performed at selected locations in the grain interior as well as grain boundaries of the MnO_2-doped sample as shown in Fig. 10(c) indicated that the Mn was located mainly at grain boundary regions. The EDAX signatures of the grain interior (not shown in the figure) registered peaks belonging to Zr, Y and O. Similar observations have been reported by Ciacchi et al. [51] for commercial 8 mol% Y_2O_3–ZrO_2 which had a high concentration of silica in the starting powders. SEM analysis performed on these samples revealed the presence of a glassy phase at the surface with occasionally specks of other phases present [52].

Considering the experimental evidence presented by the various authors and in light of the results presented in this research, it is postulated that transient liquid phase sintering was the most favourable sintering mechanism for the MnO_2-doped Y-TZP system. The first effect of MnO_2 addition on the sintering behaviour of Y-TZP is the fact that the onset temperature for densification and the required sintering holding time are lower. The improved densification can be attributed to the dissolution of MnO_2 in the Y-TZP matrix by forming Mn-rich grain boundaries in the zirconia grains, which increases the ionic mobility of Zr^{4+} within and across the grain boundary region. This significantly activate the grain boundary diffusivity and therefore facilitating particles consolidation to proceed at lower sintering temperature and sintering holding time when compared to the case of undoped Y-TZP which required higher sintering temperature and longer sintering holding time.

The XRD analysis indicates that the lattice parameters of the MnO_2-doped Y-TZP were not altered when compared to the undoped Y-TZP throughout the sintering regime employed. For

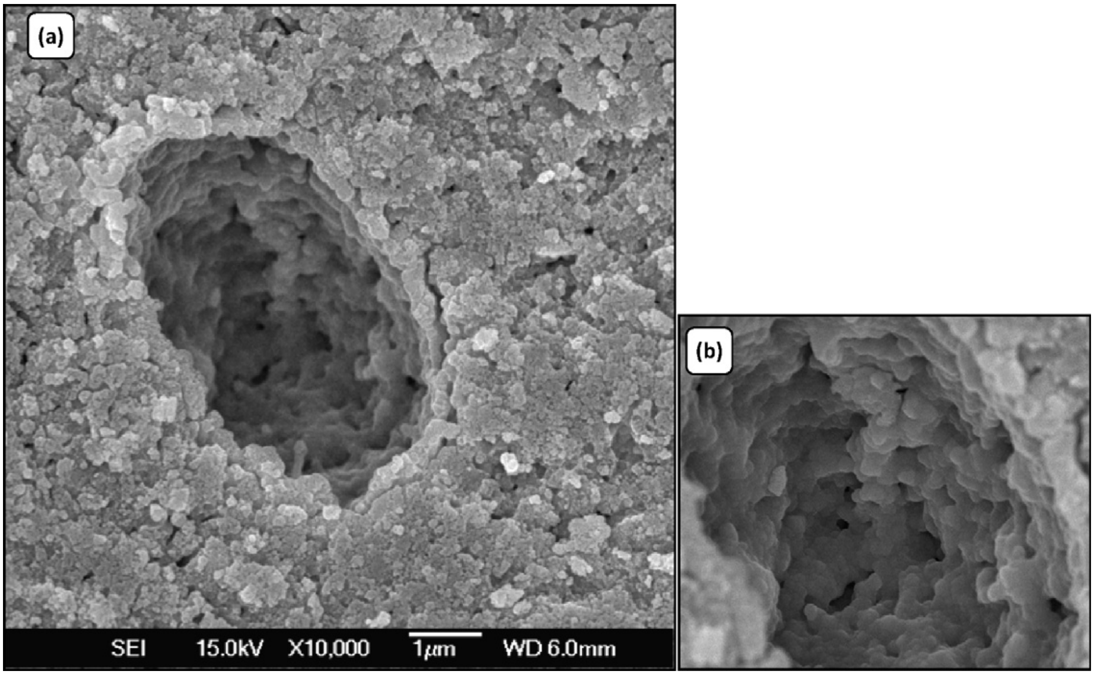

Fig. 9. (a) SEM micrograph of unpolished fracture surface of MnO_2-doped Y-TZP that was rapidly quenched from 1150 °C revealing strong features of a liquid phase sintering. (b) A close up view of the pore surface morphology.

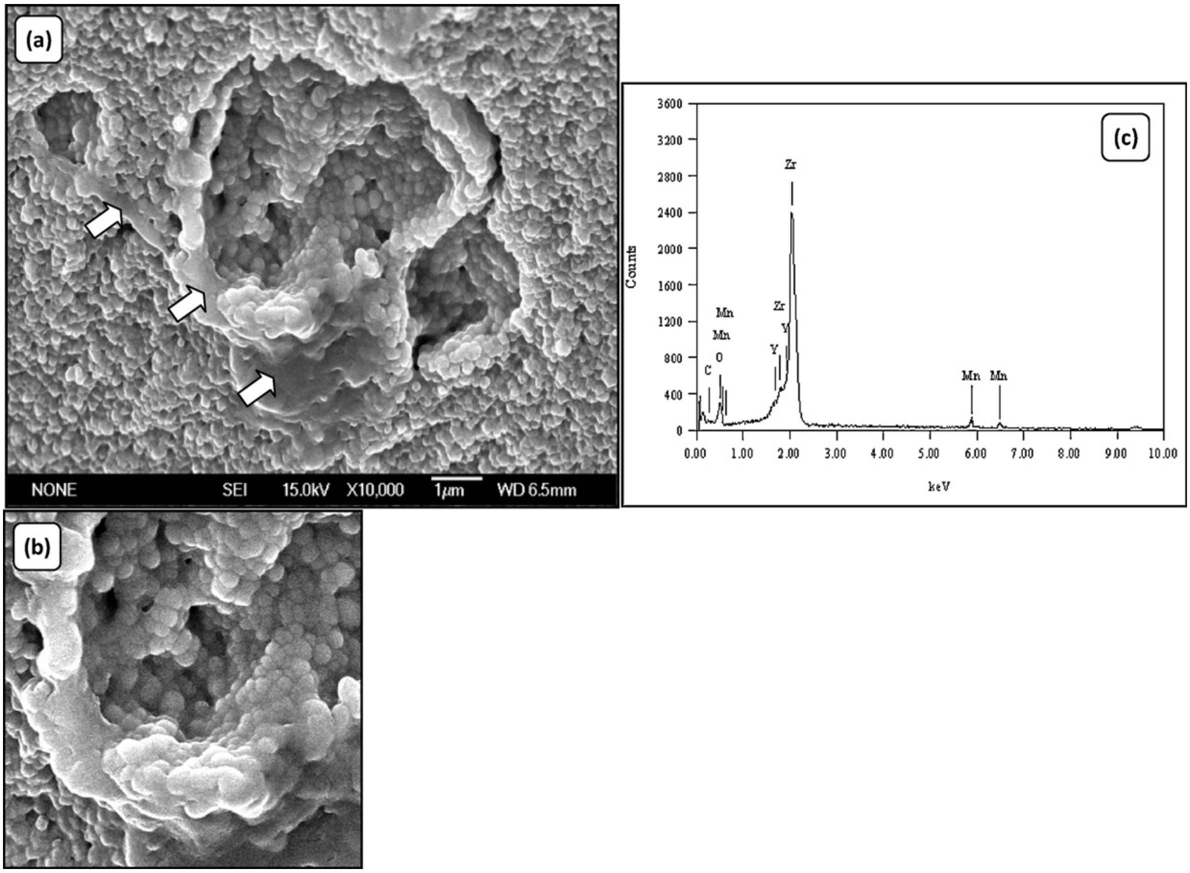

Fig. 10. (a) SEM micrograph of unpolished fracture surface of MnO_2-doped Y-TZP that was rapidly quenched from 1350 °C. The arrows indicate the solidified remnant liquid surrounding the zirconia grains. (b) Close up view revealing rounding of grains due to the effect of liquid phase. (c) EDAX analysis at the grain boundary of the MnO_2-doped Y-TZP that was rapidly quenched.

instance, the *d*-spacing for samples sintered at 1150 °C was 0.2958 nm and 0.2956 nm for the undoped and 1 wt% MnO_2-doped Y-TZP, respectively. Therefore, this result suggests that solid-solution formation between MnO_2 and Y-TZP may be negligible in the MnO_2–Y-TZP system. This is in agreement with the work of Kimura et al. [27] who reported that manganese oxide dissociate to form Mn_3O_4 when Y-TZP was sintered above 900 °C. The authors suggested that a thin Mn-rich segregation layer which cannot be detected by SEM or TEM existed in the grain boundaries.

In the present work, the XRD analysis revealed that a pronounced tetragonal to monoclinic phase transformation occurred above 1500 °C sintering. This phenomenon could be explained by the severe depletion of yttria in the zirconia grains, which is caused by the reaction between MnO_2 and yttria that has been depleted from the zirconia grains resulting in a thermodynamically instable tetragonal phase.

5. Conclusions

In the present work the effects of sintering temperature and holding time on sinterability and mechanical properties of 1 wt% MnO_2-doped Y-TZP ceramics were studied. The MnO_2-doped Y-TZPs achieved relatively high density above 95% of theoretical value when sintered at 1250 °C, approximately 100 °C lower than the temperature required to achieve the same for the undoped Y-TZP. Due to the presences of a transient liquid during the sintering of the 1 wt% MnO_2-doped Y-TZP, a shorter sintering holding time, i.e. 12-min hold, was found to be beneficial in aiding densification without sacrificing tetragonal phase stability or mechanical properties. Indication of the presence of a transient liquid phase during sintering in the MnO_2-doped system has been revealed by SEM examination of the rapidly quenched samples. A sintering mechanism involving the reaction between MnO_2 and Y_2O_3 forming a reactive liquid at the sintering temperature has been proposed for the MnO_2-doped Y-TZP system.

Acknowledgment

The authors would like to express thanks to the Ministry of Science, Technology and Innovation of Malaysia for providing the financial support.

References

[1] I. Nettleship, R. Steven, Tetragonal zirconia polycrystals (TZP)—a review, Int. J. High Tech. Ceram. 3 (1987) 1–32.
[2] J.J. Xue, Martensitic transformation in zirconia containing ceramics and its applications, Curr. Opin. Solid State Mater. Sci. 9 (2005) 313–318.

[3] R.H.J. Hannink, M.V. Swain, Progress in transformation toughening of ceramics, Ann. Rev. Mater. Sci. 24 (1994) 359–408.

[4] G.Y. Akimov, V.M. Timchenko, Mechanical properties of ceramics prepared from a nanocrystalline ZrO_2–3 mol% Y_2O_3 powder, Refract. Ind. Ceram. 45 (2004) 55–57.

'[5] S. Ramesh, C. Gill, S. Lawson, G.P. Dransfield, The effect of copper oxide on sintering, microstructure, mechanical properties and hydrothermal ageing of coated 2.5Y-TZP ceramics, J. Mater. Sci. 34 (1999) 5457–5467.

[6] B. Bikramjit, J. Vleugels, O. Van der Biest, Toughness tailoring of yttria-doped zirconia ceramics, Mater. Sci. Eng. A 380 (2004) 215–221.

[7] B. Bikramjit, J. Vleugels, O. Van der Biest, Microstructure–toughness–wear relationship of tetragonal zirconia ceramics, J. Eur. Ceram. Soc. 24 (2004) 2031–2040.

[8] R. Stevens, Zirconia and Zirconia Ceramics, Magnesium Elektron Ltd., UK, 1986, pp. 1–56 (Publ. No. 113).

[9] R.H.J. Hannink, P.M. Kelly, B.C. Muddle, Transformation toughening in zirconia containing ceramics, J. Am. Ceram. Soc. 83 (2000) 461–487.

[10] M.E. Woods, I. Oda, PSZ ceramics for adiabatic engine components, SAE Technical Paper No. 820429 (1982).

[11] S. Wada, Ceramics application for automotive components, in: S. Saito (Ed.), Advanced Ceramics, Oxford Univ. Press, UK, 1988, pp. 227–239.

[12] C. Piconi, G. Maccauro, Zirconia as a ceramic biomaterial, Biomaterials 20 (1999) 1–25.

[13] P. Pittayachawan, A. McDonald, A. Petrie, J.C. Knowles, The biaxial flexural strength and fatigue property of Lava^{TM} Y-TZP dental ceramic, Dent. Mater. 23 (2007) 1018–1029.

[14] S.P.S. Badwal, J. Drennan, Evaluation of conducting properties of yttria zirconia wafers, Solid State Ionics 40/41 (1990) 869–873.

[15] J.F. Baumard, P. Abelard, Defect structure and transport properties of ZrO_2-based solid electrolytes, in: N. Claussen, M. Ruhle, A.H. Heuer (Eds.), Advances in Ceramics, vol. 12, The Am. Ceram. Soc, Columbus, OH, 1984, pp. 555–571.

[16] S.P.S. Badwal, K. Foger, Solid oxide electrolyte fuel cell review, Ceram. Inter. 22 (1996) 257–265.

[17] M.J. Murray, S.P.S. Badwal, Solid electrolyte cell technology based on zirconia, Mater. Sci. Forum 34–36 (1988) 213–217.

[18] Z. Lu, Y. Yu, R. Guo, H. Li, Q. Guo, Influence of t-ZrO_2 addition on mechanical property and electrical conductivity of YSZ electrolyte, Rare Metals 25 (2006) 378–383.

[19] W. Dworak, D. Fingerle, Ceramics materials for engines, Ceram. Trans. J. 86 (1987) 170–182.

[20] C. Aksel, Mechanical properties and thermal shock behaviour of alumina–mullite–zirconia and alumina–mullite refractory materials by slip casting, Ceram. Inter. 29 (2003) 311–316.

[21] A.M. Anthony, High temperature refractory applications of zirconia, in: A.H. Heuer, L.W. Hobbs (Eds.), Advances in Ceramic, vol. 3, The Am. Ceram. Soc., Inc., Columbus. OH, 1981, pp. 437–454.

[22] N. Claussen, Strengthening strategies for ZrO_2 toughened ceramics at high temperatures, Mat. Sci. Eng. 71 (1985) 23–38.

[23] J.L. Federer, High temperature corrosion of heat exchanger materials, in: R.E. Tressler, M. McNallan (Eds.), Ceramics Transactions, vol. 10, The Am. Ceram. Soc. Inc., Westerville, OH, 1990, pp. 425–443.

[24] S. Moore, Ceramics die speed extrusion saves energy, Mod. Plast. 71 (1994) 37.

[25] T.K. Gupta, F.F. Lang, J.H. Bechtold, Effect of stress-induced phase transformation on the properties of polycrystalline zirconia-containing tetragonal phase, J. Mater. Sci. 13 (1978) 1464–1470.

[26] M.F. Ashby, D.R.H. Jones, Engineering Materials 2, an Introduction to Microstructures, Processing and Design, Pergamon Press Ltd., 1986, pp. 150–151.

[27] N. Kimura, S. Abe, J. Morishita, H. Okamura, Low-temperature sintering of Y-TZP and Y-TZP–Al_2O_3 composites with transitional metal oxide additives, in: S. Somiya (Ed.), Sintering 88', vol. 2, Elsevier Applied Science, 1988, pp. 1142–1148.

[28] S. Ramesh, C. Gill, Environmental degradation of CuO-doped Y-TZP ceramics, Ceram. Inter. 27 (2001) 705–711.

[29] C.-M.J. Hwang, I.-W. Chen, Effect of a liquid phase on superplasticity of 2 mol%-Y_2O_3-stabilised tetragonal zirconia polycrystals, J. Am. Ceram. Soc. 73 (1990) 1626–1632.

[30] L.A. Xue, Enhanced superplastic deformation of 2 mol% yttria-stabilised tetragonal zirconia polycrystals-alumina composite by liquid-forming additives, J. Mater. Sci. Lett. 10 (1991) 1291–1292.

[31] J.R. Seidensticker, M.J. Mayo, Thermal analysis of 3-mol%-yttria-stabilised tetragonal zirconia powder doped with copper oxide, J. Am. Ceram. Soc. 79 (1996) 401–406.

[32] W. Hendrix, S. Kuypers, J. Vangrunderbeek, J. Luyten, W. Vandermeulen, Superplasticity of CuO-doped ZrO_2 (Y_2O_3), Mater. Sci. Eng. A 168 (1993) 45–47.

[33] S. Lawson, C. Gill, G.P. Dransfield, The effects of copper and iron oxide additions on the sintering and properties of Y-TZP, J. Mater. Sci. 30 (1995) 3057–3060.

[34] S. Ran, A.J.A. Winnubst, W. Wiratha, H.A. Dave, Synthesis, sintering and microstructure of 3Y-TZP/CuO nano-powder composites, J. Eur. Ceram. Soc. 26 (2006) 391–396.

[35] S. Ran, A.J.A. Winnubst, H. Koster, P.J. de Veen, D.H.A. Blank, Sintering behaviour and microstructure of 3Y-TZP + 8 mol% CuO nano-powder composite, J. Eur. Ceram. Soc. 27 (2007) 683–687.

[36] S. Ramesh, S. Meenaloshini, C.Y. Tan, W.J. Kelvin Chew, W.D. Teng, Effect of manganese oxide on the sintered properties and low temperature degradation of Y-TZP ceramics, Ceram. Inter. 34 (2008) 1603–1608.

[37] S. Ramesh, C. Gill, S. Lawson, G.P. Dransfield, Sintering, microstructure and mechanical properties of commercial Y-TZPs, J. Mater. Sci. 31 (1996) 6055–6062.

[38] ASTM Standard C1259-2008e1, Standard test method for dynamic young's modulus, shear modulus, and poisson's ratio for advanced ceramics by impulse excitation of vibration, in: ASTM International, West Conshohocken, PA, 2008.

[39] K. Niihara, R. Morena, D.P.H. Hasselman, Evaluation of K_{Ic} of brittle solids by the indentation method with low crack-to-indent ratios, J. Mater. Sci. Lett. 1 (1982) 13–16.

[40] H. Toraya, M. Yoshimura, S. Somiya, Calibration curve for quantitative analysis of the monoclinic-tetragonal ZrO_2 system by x-ray diffraction, J. Am. Ceram. Soc. 67 (1984) C-119–C-121.

[41] A. Paterson, R. Stevens, Phase analysis of sintered yttria-zirconia ceramics by x-ray diffraction, J. Mater. Res. 1 (1986) 295–299.

[42] M.I. Mendelson, Average grain size in polycrystalline ceramics, J. Am. Ceram. Soc. 52 (1969) 443–446.

[43] B.D. Culity, S.R. Stock, Elements of X-Ray Diffraction, 3rd ed., Prentice Hall Inc., 2001, pp. 167–170.

[44] Y. Sakka, T. Ishii, T.S. Suzuki, K. Morita, K. Hiraga, Fabrication of high-strain rate superplastic yttria-doped zirconia polycrystals by adding manganese and aluminum oxides, J. Eur. Ceram. Soc. 24 (2004) 449–453.

[45] H. Erkalfa, Z. Misirli, T. Baykara, The effect of TiO_2 and MnO_2 on densification and microstructural development of alumina, Ceram. Inter. 24 (1998) 81–90.

[46] T. Zhang, P. Hing, H. Huang, J. Kilner, Sintering and densification behaviour of Mn-doped CeO_2, Mater. Sci. Eng. B 83 (2001) 235–241.

[47] S. Shimada, K. Kodaira, T. Matsushita, Sintering $LiTaO_3$ and $KTaO_3$ with the aid of manganese oxide, J. Mater. Sci. 19 (1984) 1385–1390.

[48] S.N.B. Hodgson, J. Cawley, M. Clubley, The role of Al_2O_3 impurities on the microstructure and properties of Y-TZP, J. Mater. Process. Technol. 92–93 (1999) 85–90.

[49] S.N.B. Hodgson, J. Cawley, M. Clubley, The role of SiO_2 impurities in the microstructure and properties of Y-TZP, J. Mater. Process. Technol. 86 (1999) 139–145.

[50] D.J. Kim, Effect of Ta_2O_5, Nb_2O_5 and HfO_2 alloying on the transformability of Y_2O_3-stabilized tetragonal ZrO_2, J. Am. Ceram. Soc. 73 (1990) 115–120.

[51] T.F. Ciacchi, K.M. Cran, S.P.S. Badwal, Evaluation of commercial zirconia powders for solid oxide fuel cells, Solid State Ionics 73 (1994) 49–61.

[52] G.S.A.M. Theunissen, A.J.A. Winnubst, A.J. Burggraaf, Segregation aspects in the ZrO_2–Y_2O_3 ceramic system, J. Mater. Sci. Lett. 8 (1989) 55–57.